Characterization of Noise in Digital Photographs for Image Processing

Suk Hwan Lim

HP Laboratories
HPL-2008-159

Keyword(s):
Noise model, Image processing, Imaging pipeline, correlated noise, signal-dependant noise, denoising, noise filtering

Abstract:
Many conventional image processing algorithms such as noise filtering, sharpening and deblurring, assume a noise model of Additive White Gaussian Noise (AWGN) with constant standard deviation throughout the image. However, this noise model does not hold for images captured from typical imaging devices such as digital cameras, scanners and camera-phones. The raw data from the image sensor goes through several image processing steps such as demosaicing, color correction, gamma correction and JPEG compression, and thus, the noise characteristics in the final JPEG image deviates significantly from the widely-used AWGN noise model. Thus, when the image processing algorithms are applied to the digital photographs, they may not provide optimal image quality after the image processing due to the inaccurate noise model. In this paper, we propose a noise model that better fits the images captured from typical imaging devices and describe a simple method to extract necessary parameters directly from the images without any prior knowledge of imaging pipeline algorithms implemented in the imaging devices. We show experimental results of the noise parameters extracted from the raw and processed digital images.

External Posting Date: October 21, 2008 [Fulltext] Approved for External Publication
Internal Posting Date: October 21, 2008 [Fulltext]

To be published in IS&T/SPIE Electronic Imaging, Vol. 6069

Characterization of Noise in Digital Photographs for Image Processing

SukHwan Lim
Hewlett-Packard Laboratories
1501 Page Mill Rd, Palo Alto, CA 94304

ABSTRACT

Many conventional image processing algorithms such as noise filtering, sharpening and deblurring, assume a noise model of Additive White Gaussian Noise (AWGN) with constant standard deviation throughout the image. However, this noise model does not hold for images captured from typical imaging devices such as digital cameras, scanners and camera-phones. The raw data from the image sensor goes through several image processing steps such as demosaicing, color correction, gamma correction and JPEG compression, and thus, the noise characteristics in the final JPEG image deviates significantly from the widely-used AWGN noise model. Thus, when the image processing algorithms are applied to the digital photographs, they may not provide optimal image quality after the image processing due to the inaccurate noise model. In this paper, we propose a noise model that better fits the images captured from typical imaging devices and describe a simple method to extract necessary parameters directly from the images without any prior knowledge of imaging pipeline algorithms implemented in the imaging devices. We show experimental results of the noise parameters extracted from the raw and processed digital images.

1. INTRODUCTION

Digital imaging devices such as digital cameras or camera-phones are becoming very popular and ubiquitous. More and more people are capturing many digital photographs and the number of digital photographs taken is increasing rapidly. The overall quality of images taken by many of these imagers, however, is not always satisfactory. Many digital cameras or camera phones today provide poor quality shots in low illuminations such as indoors or night situations. It is very difficult to capture good quality photographs in these situations since elongating exposure time increases motion blur and shortening exposure time reduces the signal-to-noise-ratio (SNR). Image sensors in digital cameras typically lack the dynamic range and sensitivity to capture both the dark and bright parts of the scene. In many cases, auto-exposure algorithm sets the exposure time such that the bright region is not overly saturated, leaving the dark region grossly under-exposed. Such pictures have very poor signal-to-noise-ratio (SNR) due to lack of captured photons. There are other scenarios, when even carefully planned shots are underexposed, such as in museums where flash is not permitted, or when taking a picture of a moving object at high ISO settings. In addition, low quality optics and sensors are included in many consumer devices, such as camera phones and PDAs. These devices are typically used to take unplanned casual shots, potentially in bad lighting conditions that induce increased noise. Furthermore, many of these devices do not have built-in-flash, making it nearly impossible to capture good quality shots in low light situations.

Digital cameras and camera phones have always been in a Mega-pixel war from the very early introduction. Since the consumers almost always prefer higher number of pixels, this trend is expected to continue into the future although higher pixel count will not automatically translate into better image quality. Since the die (chip) size of the image sensors remain relatively constant due to the constraints set by the optics and cost, the area allocated for each pixel will decrease if the trend of increasing pixel count continues.[1] Although higher pixel count will result in higher spatial resolution, it is detrimental to signal integrity at each pixel because each pixel will receive less light (photons) and generate less charge. The size of the individual pixel sensors has been shrinking to accomodate the large mega-pixel counts that the consumers demand, and these tiny pixels can only catch a small number of photons. As will be elaborated in Section 2, less charge captured results in lower SNR and hence lower image quality. This provides higher challenge for subsequent image processing algorithms to produce good quality photographs. Thus, it is important to understand the characteristics of noise in order to produce high quality photos from the images with low SNR. Note that sub-optimal image processing in the imaging devices can contribute to lower image quality as well.

Many image processing algorithms such as sharpening, contrast enhancement and noise filtering are developed and tested under the assumption of Additive-White-Gaussian-Noise (AWGN) with constant standard deviation across the

image. However, this noise model is not adequate for images captured from digital cameras, scanners and cell-phone imagers. Thus, when the image processing algorithms are applied to the digital photographs, they cannot fully exploit the characteristics of noise and may not provide optimal image quality after processing due to inaccurate noise model. Specifically, unprocessed raw data captured straight from the image sensors contain white noise but the standard deviation of the noise is not constant. Furthermore, the raw image goes through several image processing steps such as demosaicing, color correction, gamma correction, color transformation and JPEG compression, and thus, the noise characteristics in the final output image deviate significantly from the widely-used AWGN noise model. In this paper, we propose a noise model that better fits the images captured from typical imaging devices and describe a method to extract necessary parameters directly from the images without prior knowledge of image processing algorithms implemented in the imaging devices. We show experimental results of the noise parameters extracted from the images and discuss how it can be used for image processing algorithms.

2. NOISE MODEL FOR IMAGE SENSORS AND SIMPLE IMAGING PIPELINE

In this section, we review the noise model for the image sensor and describe how the noise characteristics are modified with each step in the imaging pipeline of the digital cameras or camera phones. In general, the specific algorithms in the imaging pipeline are not publicly disclosed for most imaging devices although the overall architecture does not vary significantly from one device to another. We define an imaging pipeline that is general and simple for our analysis. Although the analysis may not be accurate for more sophisticated imaging devices, it allows us to make approximate predictions on the noise characteristics seen in the digital photographs.

2.1 Noise model for image sensors

In this subsection, we review the noise model for image sensors. More detailed analyses and descriptions can be found in many papers included in the reference[1, 2, 3, 4, 5]. Since the image quality heavily depends on the image sensors, it is important to examine the model of image sensors. When photons (light) hit the photo-element in each pixel, they generate photocurrent. During capture, each pixel converts incident light into photocurrent i_{ph} for the duration of exposure time T such that the accumulated signal charge, Q_{sig}, is

$$Q_{sig} = i_{ph}T,$$

assuming the pixel is not saturated. Note that the signal charge is directly proportional to the light intensity at each pixel. In addition to the signal charge, the accumulated dark current and the additive noise terms are added to this charge and the total charge, Q_{tot}, can be expressed as

$$Q_{tot} = Q_{sig} + i_{dc}T + N_{lin} + N_{sq} + N_{offset},$$

where i_{dc} is the dark current, N_{lin} is the shot noise term whose variance monotonically increases with the accumulated signal charge, N_{offset} is the aggregate of noise terms whose total variance is constant regardless of the signal charge, and N_{sq} is the gain fixed pattern noise whose variance increases as a quadratic function of the accumulated signal charge. Sources for N_{offset} include readout noise, reset noise, quantization noise, shot noise of the dark current and offset fixed pattern noise. In summary, the variance of the noise terms are

$$\sigma_{lin}^2 = qi_{ph}T = qQ_{sig}$$
$$\sigma_{sq}^2 = k_1 (i_{ph}T)^2 = k_1 Q_{sig}^2$$
$$\sigma_{offset}^2 = k_0$$

,where k_0 and k_1 are constants and q is the electron charge. The total noise variance is

$$\sigma_{tot}^2 = k_0 + k_1 Q_{sig}^2 + qQ_{sig}. \quad (1)$$

It can be seen that the total noise variance is not a constant but a 2nd order polynomial function with respect to Q_{sig}. As q, k_0 and k_1 are non-negative values, the noise variance increases with the signal charge at each pixel. It can be seen in Figure 1 which shows a plot of the noise standard-deviation (STD) versus signal charge. Although the noise variance is larger for higher pixel intensities, the signal quality is actually higher for high intensities. The SNR can be computed as

$$\text{SNR} = Q_{sig}^2 / (k_0 + k_1 Q_{sig}^2 + qQ_{sig}).$$

An example of SNR versus light intensity curve is shown in Figure 1. Note that the SNR is low and the signal integrity is poor when the pixels are not able to capture enough photons (i.e. dark scenes). This can cause huge problems for image quality due to very low SNR. When more photons can be captured by increasing the overall light intensity or elongating the exposure time, the SNR is increased. However, it is generally not possible to control the overall light intensity for most environments and there is a limit to extending the exposure time due to motion blur. Thus, the image quality problem is the most difficult to cope with under bad illuminations such as indoors or night times.

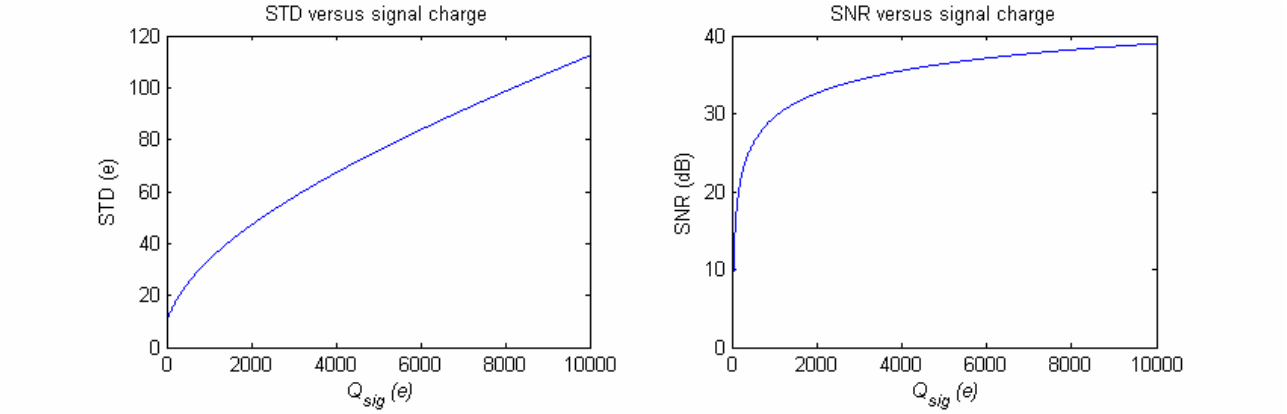

Figure 1: Noise variance and SNR versus pixel intensity

Although the assumption of constant standard-deviation is not valid for the noise in image sensors, the conventional assumption of AWGN generally holds for the raw data captured from the image sensor[5]. The total noise has a probability density function that is very close to a Gaussian distribution and the assumption of white noise also holds. The noise at each pixel is independent of the noise in the neighboring pixels, so the auto-correlation function of the noise in the image sensor is

$$R_N(i, j) = \begin{cases} \sigma_{tot}^2 & i = 0, j = 0 \\ 0 & otherwise \end{cases} \qquad (2)$$

2.2 Noise model for imaging pipeline

In this subsection, we describe how the noise characteristics are modified at various stages of the imaging pipeline. We show that the assumption of AWGN is not valid after the raw data goes through the imaging pipeline of the imaging device. A simple imaging pipeline is defined for the purpose of analyzing the noise characteristics. Note that most imaging pipeline are more sophisticated than the simple pipeline, but are much more difficult to predict analytically how the noise characteristics are modified throughout the pipeline.

A block diagram of a typical imaging pipeline[5, 6, 7, 8, 9] for a digital camera or camcorder is shown in Figure 2. Since the image sensors typically have Bayer pattern overlaid on top of the image sensor, each pixel only captures the intensity for one color channel. Thus, demosaicing is performed to interpolate missing color channels at each pixel. (For example, if a pixel only captures green color channel, the blue and red color channels should be interpolated from the neighboring pixels.) Then, color correction is performed as the color space of the image sensor does not match that of a color standard or a nominal display. Typically, color correction is performed with a 3x3 matrix multiplication at each pixel. After color correction, in order to compensate for the non-linearity of the displays, the RGB signals are gamma corrected. Gamma correction is typically performed by applying a pre-defined one-to-one mapping function to the pixel intensities and is implemented with a table look-up. Then, the RGB values are transformed to luminance (Y) and Chrominance (Cb and Cr) values via multiplication of a 3x3 color transformation matrix. Most cameras apply JPEG compression to the YCbCr values where the Cb and Cr values are typically downsampled by 2 (both horizontally and vertically) and highly quantized.

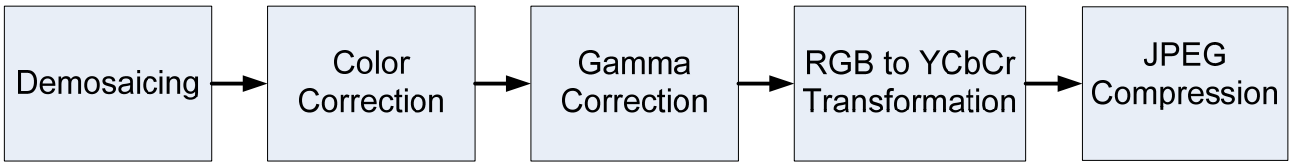

Figure 2: A simple imaging pipeline.

2.2.1 Demosaicing

As mentioned previously, demosaicing is performed to interpolate missing color channels at each pixel. Demosaicing is essentially a spatial interpolation algorithm where inter-channel correlations can be exploited to enhance the image quality. When a Bayer pattern is overlaid on top of the image sensor, a 2 x 2 spatial interpolation should be performed on the red and blue channels and the number of pixels should be increased by 2 for the green channel. Many methods have been developed for demosaicing and survey papers on this topic can be found in the reference.[10, 11, 12, 13]

Consider the Bayer pattern unit in Figure 3. Each pixel only captures one color channel and demosaicing computes the other two missing color channels at the pixel. For example, in pixel 1, the pixel only captures the red color channel and the blue and green intensity values must be interpolated using the neighborhood.

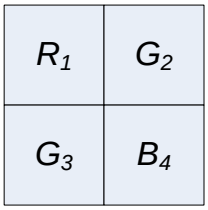

Figure 3: A unit Bayer pattern.

In our simple imaging pipeline, we assume a simple nearest neighbor replication for demosaicing. With this simple scheme, the intensity values are copied to the neighboring pixels. i.e.,

$$\hat{R}_2 = \hat{R}_3 = \hat{R}_4 = R_1$$
$$\hat{G}_1 = G_3, \quad \hat{G}_4 = G_2$$
$$\hat{B}_1 = \hat{B}_2 = \hat{B}_3 = B_4$$

When the noise goes through the demosaicing step, the noise characteristics are modified. Although the noise variance does not change, spatial characteristics of the noise after demosaicing are modified. Specifically, the auto-correlation of the noise at each color channel is not the same as Equation (2) any more. For red and blue channel, the auto-correlation of the noise is

$$R_{NR}(i,j) = \begin{cases} \sigma^2 & i=0,\ j=0 \\ \frac{1}{2}\sigma^2 & i=\pm 1,\ j=0 \\ \frac{1}{2}\sigma^2 & i=0,\ j=\pm 1 \\ \frac{1}{4}\sigma^2 & i=\pm 1,\ j=\pm 1 \\ 0 & otherwise \end{cases},$$

where σ is the total standard deviation of noise. For the green channel, the auto-correlation of the noise is

$$R_{NG}(i,j) = \begin{cases} \sigma^2 & i=0,\ j=0 \\ \frac{1}{2}\sigma^2 & i=0,\ j=\pm 1 \\ 0 & otherwise \end{cases},$$

Note that the noise now has some spatial correlation and that the low frequencies have higher power spectral density than the high frequencies. Thus, the noise is not white noise any more, but is colored.

2.2.2 Color Correction

$$\begin{bmatrix} R_{out} \\ G_{out} \\ B_{out} \end{bmatrix} = \begin{bmatrix} c_{11} & c_{12} & c_{13} \\ c_{21} & c_{22} & c_{23} \\ c_{31} & c_{32} & c_{33} \end{bmatrix} \begin{bmatrix} R_{in} \\ G_{in} \\ B_{in} \end{bmatrix}$$

Color correction is typically implemented with a 3x3 matrix multiplication shown above. The elements of the matrix depend on the spectral response of the image sensor and the color filters. When color correction is applied, noise also goes through the matrix multiplication and the noise variance is changed as follows:

$$\sigma^2_{NRout} = c^2_{11}\sigma^2_{NRin} + c^2_{12}\sigma^2_{NGin} + c^2_{13}\sigma^2_{NBin}$$
$$\sigma^2_{NGout} = c^2_{21}\sigma^2_{NRin} + c^2_{22}\sigma^2_{NGin} + c^2_{23}\sigma^2_{NBin}$$
$$\sigma^2_{NBout} = c^2_{31}\sigma^2_{NRin} + c^2_{32}\sigma^2_{NGin} + c^2_{33}\sigma^2_{NBin}$$

For typical color correction, the noise variance does not change significantly. However, the SNR is degraded when there are significant off-diagonal negative elements as the signal strength is decreased.[14, 15, 16, 17] This occurs when the spectral response of the color filters have high correlation. The spatial characteristics of the noise are not altered significantly as the color correction is a pixel-wise operation.

2.2.3 Gamma correction and contrast enhancement

Gamma correction is applied to the color corrected R, G and B values. Typically, the intensity values go through a mapping function [6, 7, 8, 9, 18]

$$I_{out} = \alpha\left(\frac{I_{in}}{\beta}\right)^{\gamma} = f(I_{in}) \qquad (3)$$

where α, β and γ are constants, I_{in} is the input prior to gamma correction and I_{out} is the output. To analyze the change in the noise standard-deviation (STD), we make a linear approximation. If we assume that the noise is typically much smaller than signal, then

$$I_{out} = \left(\left.\frac{df(I_{in})}{dI_{in}}\right|_{I_{in}=I_0}\right)(I_{in} - I_0) + f(I_0)$$

for intensities near I_0. If the noise standard deviation is σ_{Nin} for intensities near I_0, then the standard deviation, σ_{Nout}, after gamma correction for intensities near $f(I_0)$ is equal to

$$\sigma_{Nout} = \left(\left.\frac{df(I_{in})}{dI_{in}}\right|_{I_{in}=I_0}\right)\cdot\sigma_{Nin}(I_0) = \frac{\alpha\gamma}{\beta}\left(\frac{I_0}{\beta}\right)^{\gamma-1}\sigma_{Nin}(I_0) \qquad (4)$$

Note that the noise is either amplified or suppressed depending on the slope of the mapping function $f()$ at I_0. For typical gamma correction where $\gamma = 2.2$ in Equation (3), the noise standard deviation is decreased for dark regions and is

increased for bright regions. It is worthwhile to point out that this analysis can be applied to any pixel-wise mapping operation. Many types of contrast enhancement can be analyzed similarly with the use of Equation (4).

2.2.4 RGB to YCbCr conversion and image compression

In most digital cameras and camera phones, RGB values are converted to YCbCr values prior to JPEG compression. The color transformation is performed by multiplying a 3x3 matrix to the R, G and B values. The operation is identical to the color correction in subsection 2.2.2 except for the differences in the specific values of the elements in the 3x3 matrix. A typical RGB to YCbCr conversion is

$$\begin{bmatrix} Y \\ Cb \\ Cr \end{bmatrix} = \begin{bmatrix} 0.299 & 0.587 & 0.114 \\ -0.169 & -0.331 & 0.500 \\ 0.500 & -0.419 & -0.081 \end{bmatrix} \begin{bmatrix} R \\ G \\ B \end{bmatrix}$$

It is worthwhile to point out that the SNR for the chrominance (Cb and Cr) channels are typically much lower than that of the luminance channel. The degradation of the SNR for the chrominance channels is mostly due to the reduction in signal energy. Note that the degradation depends on the correlation of the R, G, and B channels. The negative elements of the color transformation matrix reduce the signal strength while the noise strength is relatively unchanged.

After the R, G and B values are transformed to Y, Cb and Cr values, the color channels are compressed independently. The image is divided into non-overlapping 8x8 blocks and 2D-DCT is performed on each block. The 2D-DCT coefficients are then quantized and the quantized values are losslessly coded with the use of run-length codes and Huffman-like codes. As the lossless step of the compression does not affect the image quality, we focus our attention to the lossy part of the compression. Typically, the high frequency components of the DCT coefficients are more coarsely quantized than the low frequency components. The energy in the high frequency is attenuated more than the low frequencies for both the signal and the noise. Thus, after JPEG compression, the noise has stronger low frequency component than the high frequency component and the noise becomes more spatially correlated. Note that this is more prominent for chrominance channels as the chrominance channels are typically downsampled spatially prior to compression. Furthermore, the chrominance channels are even more coarsely quantized than the luminance channel and the signal fidelity of the chrominance channels are more adversely affected than the luminance channel. Intuitively, JPEG compression spends far less bits on the chrominance channels than on the luminance channel, and thus, the quality of the chrominance are degraded far more than the luminance channel.

3. CHARACTERIZATION OF NOISE IN DIGITAL PHOTOGRAPHS

For most digital cameras, the imaging pipeline is not disclosed publicly and thus is not assumed to be known. Furthermore, most imaging devices employ far more sophisticated imaging pipeline that can be highly non-linear and difficult to analyze the effect on the noise characteristics. In this section, we discuss simple methods to analyze the noise characteristics directly from a digital photograph without any explicit knowledge of the imaging pipeline of the device that captured and processed the digital photograph. The profiling of the noise is aimed at providing more side information on the noise statistics for later image processing. Many image processing applications can benefit from more accurate knowledge of the noise in the image. Note that most image processing algorithms do not implicitly or explicitly assume any statistical knowledge of the noise or just assume AWGN with constant standard deviation.

The overall block diagram of analyzing the characteristics of noise is shown in Figure 4. First, the areas that mostly contain noise (but not edges or other image features) are chosen. Second, the intensities of these areas are locally curve-fitted to estimate the noise-free intensity values. Third, a noise map is found by subtracting the original image with the locally-curve-fitted image at corresponding pixel locations. Finally, the noise maps are analyzed such that various statistics of noise are estimated.

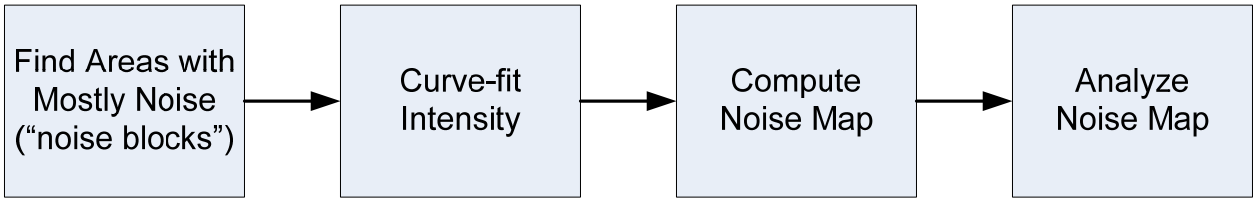

Figure 4: Block diagram of noise analysis.

To find areas that mostly contain noise (but not edges, corners or other image textures), we compute the intensity differences between all the immediate neighboring pixels in a local area. The local area can take any shape, but for simplicity of implementation, we chose to compute the intensity differences in sliding blocks. The maximum of absolute intensity differences in the block is compared to a threshold and the block is marked as a "noise block" if the maximum magnitude of the intensity differences is smaller than the threshold. A "noise block" is a block that contains little or no edges, corners or other image textures. Instead of the maximum neighboring pixel difference, other measures such as the magnitude of spatial gradients or the magnitude of Laplacians can be used as well. The threshold is a free parameter which can be computed by iterating such that adequate number of blocks are selected as "noise blocks". An initial value of the threshold can be chosen by inspecting the image sensor specifications if available.

Once the noise blocks are chosen, the intensities of these blocks are fitted with a smooth surface. In our implementation, the following model is used

$$\hat{I}(x, y) = ax + by + c\,,$$

where (x,y) are pixel locations and a, b and c are curve-fit parameters. For each block, a^*,b^* and c^* values can be found by minimizing the sum of the squared differences of the intensity value and the curve fit value. (i.e.,

$$(a^*, b^*, c^*) = \arg\min_{(a,b,c)} \sum_{(x,y)\in B} (I(x, y) - (ax + by + c))^2\,,$$

where B is the areas within "noise blocks". This equation can be solved via the least-squares method. Note that other smooth surfaces such as second order surfaces can be used at the cost of higher computational complexity. Once the curve-fits for the "noise blocks" are found, the noise map can then be computed by subtracting the actual pixel intensity values with the curve-fitted values. i.e.,

$$n(x, y) = I(x, y) - \hat{I}(x, y) = I(x, y) - (a^* x + b^* y + c^*)$$

where (x, y) is in the noise block. Once the noise map is found for all the noise blocks in the image, we can now compute simple statistics of the noise. First, we compute the noise standard-deviation and the mean intensity for each "noise block". These values are then used to compute the noise standard-deviation (STD) versus the intensity function. Second, the histogram of the noise map for each block can be analyzed for probability density function of the noise. Third, the auto-correlation of the noise can be computed by performing the spatial averaging

$$R_N(i, j) = \tfrac{1}{M} \sum_{(x,y)\in B,(x-i,y-j)\in B} n(x, y)n(x - i, y - i)\,,$$

where M is the total number of pixels used for spatial averaging. Once the auto-correlation of the noise is found, the power spectral density of the noise can be computed. This can be useful when the image is decomposed into several frequency bands prior to image processing. Note that other measures such as high-order statistics or cross-correlations can also be computed using the noise map as necessary. Also, it is worthwhile to point out that it is possible to compute these measures in any color space. For example, if the image processing is to be performed in YCbCr space, the noise statistics should be computed in the YCbCr space.

4. EXPERIMENTAL RESULT

In this section, we show some experimental result of analyzing the noise in a digital photograph. We perform two experiments. The first experiment is on the raw image data obtained from the image sensor with a Bayer pattern overlaid on top of the sensor. Due to the Bayer pattern, the red, green and blue channels are subsampled. The second experiment is on the processed image data obtained from a digital camera. Note that this image has been processed with a sophisticated imaging pipeline and the contrast was enhanced. The input images of these two experiments are shown in Figure 5.

Figure 5: Input images for experiment (left: raw image, right: processed image)

First, we show the result of analyzing a raw image before going through any imaging pipeline. We apply our noise profiling methods to show that the noise profile can be explained with the image sensor model described in Section 2.1. The results are shown in Figure 6 and Figure 7.

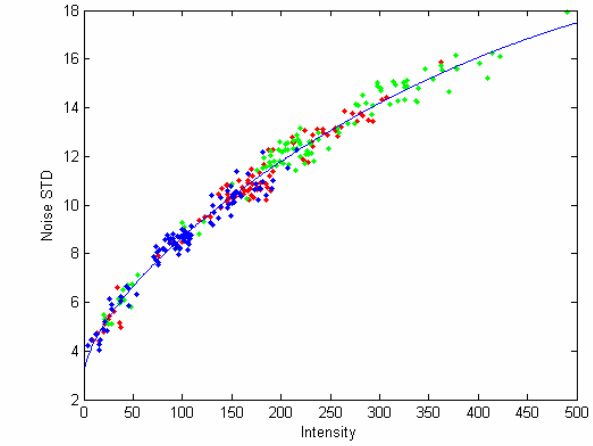

Figure 6: Noise STD versus intensity for red, blue and green channels

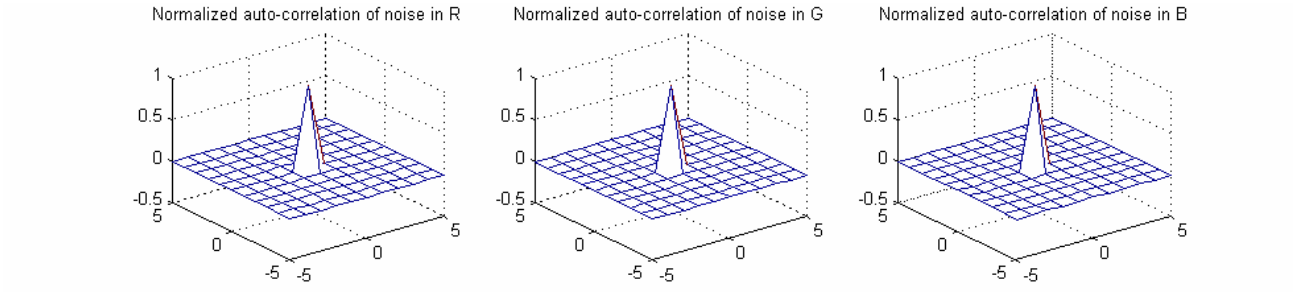

Figure 7: Auto-correlation of noise in raw R, G and B channels (prior to demosaicing)

Note that the signal versus intensity function is the same for all the color channels. This is coherent with the image sensor model as the noise STD only depends on the amount of charge captured at each pixel. The digital intensity values are directly proportional to the charge captured. It can be seen in Figure 6 that the STD increases with intensity as expected and that the shape of the function is what the noise model suggests (i.e. has a term that increases as square root of the STD). A curve-fit with the noise model in Equation (1) suggests that our noise profiling is accurate. Also, Figure 7 shows that the spatial correlation of the noise map has nonzero value only at the origin (i.e. the noise is white), which is also coherent with our image sensor noise model that assumes spatially independent noise.

In our second experiment, we show results on a digital image already passed through imaging pipeline and contrast enhancement. This photograph was captured in low illumination and the contrast of the low light areas has been enhanced significantly. It is assumed that we do not have any prior knowledge about the imaging pipeline that produced the image. The plot of noise STD versus light intensity is shown in Figure 8. It can be seen that the noise characteristics are very different from the noise model of the image sensor. As was predicted from Section 2.2, the noise STD versus intensity function is very different from the result in the first experiment (see Figure 6), due to the contrast enhancement and gamma correction steps in the imaging pipeline. Also note that the STD function is not the same for any color channels because of inter-channel operations such as color correction and color transformations in the imaging pipeline.

The normalized autocorrelation of the R, G and B channels are shown in Figure 9. It can be seen that the 2D spatial correlation has significant non-zero value outside of the origin. This means that the noise is spatially correlated and that the power spectral density of the noise is higher for lower frequencies than the higher frequencies. Also, note that the green channel has a smaller width of spatial correlation than that of the red and blue channels. Since the number of pixels for the green channel is twice the number of pixels for the red or blue channel in the Bayer pattern, the spatial interpolation in the demosaicing step can use smaller spatial support for the green channel. This leads to smaller width for the spatial correlation of noise. This is consistent with the prediction in the Subsection 2.2.1.

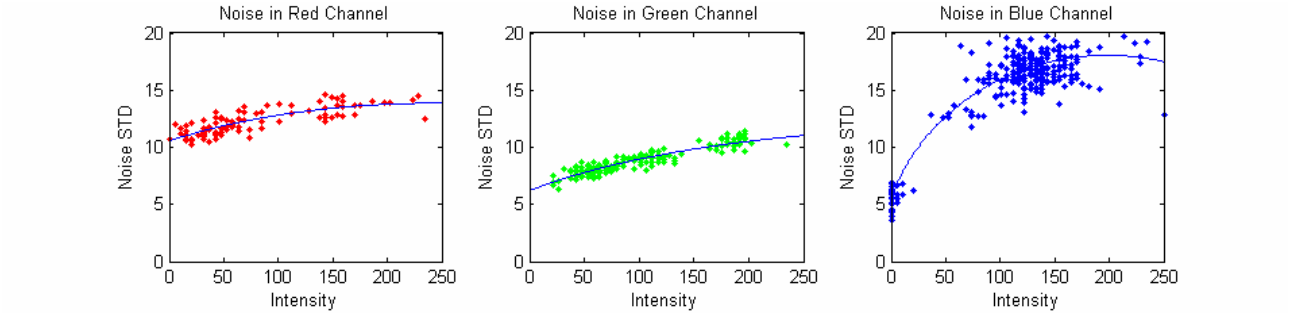

Figure 8: Noise STD versus intensity for red, green and blue channels

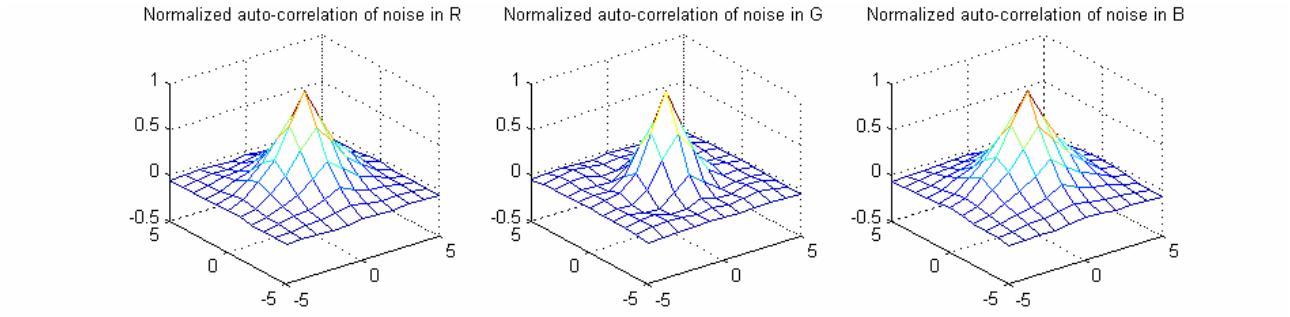

Figure 9: Auto-correlation of noise in R, G and B channels after processing

5. SUMMARY

We have shown that the conventional noise model of AWGN (with constant standard-deviation) does not hold for images obtained from typical imaging devices such as digital cameras, scanners and cell-phone imagers. We proposed a noise model that better fits the images captured from typical imaging devices and described a method to extract necessary parameters directly from the images without any prior knowledge of imaging pipeline algorithms implemented in the imaging devices. We then showed experimental results of the noise parameters extracted from the images.

REFERENCES

1. T. Chen, P. Catrysse, J. DiCarlo, A. El Gamal, B. Wandell, "How Small Should Pixel Size Be?", *Proceedings of SPIE*, vol. 3965, pp. 451-461, January 2000.
2. Hui Tian, Boyd Fowler, and Abbas El Gamal, "Analysis of Temporal Noise in CMOS APS," *Proceedings of the SPIE*, Vol. 3649, pp. 177-185, San Jose, CA, January 25-26, 1999.
3. David Yang, and Abbas El Gamal, "Comparative Analysis of SNR for Image Sensors with Enhanced Dynamic Range," *Proceedings of the SPIE*, Vol. 3649, pp. 197-211, San Jose, CA, January 25-26, 1999.
4. X. Liu and A. El Gamal, "Photocurrent Estimation from Multiple Non-destructive Samples in a CMOS Image Sensor," *Proceedings of SPIE*, Vol. 4306, pp. 450-458, January 2001.
5. A. El Gamal and P. Wong, "EE392B Class Handout" (http://www.stanford.edu/class/ee392b), Stanford University, 2005.
6. Lionel J. D'Luna et al. "A Systems approach to Custom VLSI for a Digital Color Imaging System.", *IEEE Journal of Solid-State Circuits*, 26(5):727-737, May 1991.
7. Shin-Shu Wang and Ye-Quang Chen, "A New Color Image Processor for the Video Camera", *Proceedings of the SPIE*, volume 2501, p.931-935, 1995
8. Wen-Hsin Chan and Ching-Twu Woue. "Video CCD based portable digital still camera". *IEEE Transactions on Consumer Electronics*, 41(3):455-459, Aug 1995.
9. Wen-Hsin Chan. "A mega-pixel Resolution PC Digital Still Camera". *Proceedings of the SPIE*, volume 2654, p.164-171, 1996.
10. James E. Adams, Jr. "Design of practical color filter array interpolation algorithms for digital cameras". *Proceedings of the SPIE*, volume 3028, p.117-125.
11. Michael A. Kriss, "Color Filter Arrays for Digital Electronic Still Cameras". *IS&T's 49th Annual Conference*, p.272-278, 1996.
12. Michael A. Kriss. "Digital Electronic Still Imaging: A System Analysis and Simulation". *IS&T's 49th Annual Conference*, p. 317-321, 1996.
13. Ting Chen, "A Study of Spatial Color Interpolation Algorithms for Digital Cameras", EE362 Class Project, 1999 (http://www-ise.stanford.edu/~tingchen/)
14. P. Vora and C. Herley, "Trade-offs Between Color Saturation and Noise Sensitivity in Image Sensors", in *Proceedings of the IEEE International Conference on Image Processing*, Vol. 1, pp. 196-200, 1998.
15. G. Sharma and H. J. Trussell, "Figures of Merit for Color Scanners", *IEEE Transactions on Image Processing*, Vol. 6, No. 7, pp. 990-1001, Jul 1997.
16. M. J. Vrhel, H. J. Trussell, "Filter Considerations in Color Correction", *IEEE Transactions on Image Processing*, Vol 3, No. 2, pp. 147-161, Mar 1994.
17. S.H. Lim and A. Silverstein, "Spatially Varying Color Correction (SVCC) Matrices for Reduced Noise," in *Proceedings of the 12th Color Imaging Conference*, pp. 76-81, Scottsdale, AZ, November 2004.
18. Shigeo Sakaue et al. Adaptive Gamma processing of the video cameras for the expansion of the dynamic range. *IEEE Trans. on Consumer Electronics*, 41(3): 555-561, Aug 1995.